Radiotherapy and Oncology 137 (2019) 24–31

Contents lists available at ScienceDirect

Radiotherapy and Oncology

journal homepage: www.thegreenjournal.com

Original Article

Residual gammaH2AX foci in head and neck squamous cell carcinomas as predictors for tumour radiosensitivity: Evaluation in pre-clinical xenograft models and clinical specimens

Sarah Meneceur [a,b,*], Steffen Löck [a,c,d,e], Volker Gudziol [f], Sandra Hering [g], Rebecca Bütof [a,e,h], Maximilian Rehm [a,e,h], Michael Baumann [a,b,c,d,e,h], Mechthild Krause [a,b,c,d,e,h], Cläre von Neubeck [a,c,d]

[a] OncoRay – National Center for Radiation Research in Oncology, Faculty of Medicine and University Hospital Carl Gustav Carus, Technische Universität Dresden, Helmholtz-Zentrum Dresden – Rossendorf; [b] Helmholtz-Zentrum Dresden – Rossendorf, Institute of Radiooncology – OncoRay; [c] German Cancer Consortium (DKTK), partner site Dresden; [d] German Cancer Research Center (DKFZ), Heidelberg; [e] Department of Radiotherapy and Radiation Oncology, Faculty of Medicine and University Hospital Carl Gustav Carus, Technische Universität Dresden; [f] Department of Otorhinolaryngology, Medical Faculty and University Hospital Carl Gustav Carus, Dresden; [g] Institute for Legal Medicine, Faculty of Medicine Carl Gustav Carus, Technische Universität Dresden; and [h] National Center for Tumour Diseases (NCT), partner site Dresden, Germany

ARTICLE INFO

Article history:
Received 15 December 2018
Received in revised form 3 April 2019
Accepted 4 April 2019
Available online 29 April 2019

Keywords:
γH2AX
Predictive biomarker
Radiosensitivity
HNSCC
Xenograft models
Clinical specimens

ABSTRACT

Background and purpose: Predictive biomarkers can be instrumental to treatment individualisation of cancer patients and improve therapy outcome. Residual γH2AX foci represent a promising biomarker to predict tumour radiosensitivity. In this pre-clinical study, the slope of the dose–response curve was evaluated for its predictive relevance in head and neck squamous cell carcinoma xenografts (HNSCC). Additionally, the feasibility of the translated assay was tested in a clinical setting in patient derived HNSCC samples, and associations between residual γH2AX foci and clinical parameters were analysed.

Materials and methods: Seven HNSCC xenografts models (FaDu, SAS, SKX, UT-SCC-5, UT-SCC-14, UT-SCC-45, XF354) were used. Tumour bearing NMRI nude mice were randomly distributed to five treatment arms (0–8 Gy). Residual γH2AX foci (24 h post irradiation) were counted by visual scoring in a micromilieu dependent manner (assessed with BrdU and pimonidazole). The local tumour control values measured as TCD_{50} (tumour control dose 50%) have previously been published. Patient derived HNSCC biopsies were cultivated *ex vivo* for 24 h including 4 h of pimonidazole and BrdU treatment, subsequently irradiated with 0–8 Gy and fixed after 24 h.

Results: In the pre-clinical study, the dose–response curve slopes negatively correlated with the tumour control dose after fractionated irradiation ($TCD_{50,fx}$, $R^2 = 0.63$, $p = 0.032$) and after single dose irradiation under homogeneous hypoxia ($TCD_{50,SD,clamp}$, $R^2 = 0.66$, $p = 0.027$). The γH2AX assay in clinical HNSCC samples showed a dose–response relationship, with the values of the slopes ranging from 0.099 Gy^{-1} to 0.920 Gy^{-1} (coefficient of variation = 52.8%). Slopes derived from patients were in the same ranges as the sensitive, moderate and resistant models of the pre-clinical study. Statistical analysis revealed a significant negative correlation between the slope and the patients' age ($R^2 = 0.65$, $p = 0.001$).

Conclusion: These results further support the promise of the slope of the residual γH2AX foci dose–response as a biomarker for radiosensitivity. In the clinical samples, the variation in the slopes reveals patients' specific repair capacities, which could hold potential value for treatment individualisation.

It is estimated that 50% of patients newly diagnosed with cancer will need to undergo radiotherapy [1]. Tumour response to radiotherapy varies between patients [2,3] and influences the success rate of radiotherapy. Treatment individualisation based on patient characteristics should therefore increase cure rates and reduce normal tissue complications [4]. For that matter, predictive biomarkers are of paramount importance to foresee tumour response ahead of treatment and optimise care for the patient [5].

Head and neck cancers are the 7th most common cancers in Europe [6], and approximately 91% of them are squamous cell carcinomas [7]. Standard of care for HNSCC substantially relies on radiotherapy [3]. Consequently, the establishment of a predictive biomarker for radiosensitivity in HNSCC is of high clinical relevance to optimise treatment.

Following irradiation, the phosphorylation of histone H2AX on serine 139 (called γH2AX) surrounding the DNA damage is

* Corresponding author at: OncoRay, Faculty of Medicine, Fetscherstraβe 74, 01307 Dresden, Germany.
E-mail address: sarah.meneceur@uniklinikum-dresden.de (S. Meneceur).

https://doi.org/10.1016/j.radonc.2019.04.009
0167-8140/

considered a *bona fide* marker for DNA double strand breaks (DSB) [8–11]. Since its discovery [8,9], γH2AX has therefore emerged as a powerful biomarker of radiosensitivity. Several studies demonstrated that residual γH2AX foci, which persist 24 h post-irradiation, will likely lead to cell death [12,13] and can be used to predict radiosensitivity in well oxygenated tumour regions [14–20]. Recently, the γH2AX foci assay was transferred to an *ex vivo* setting to test its clinical feasibility on tumour biopsies and evaluate inter and intra-tumoral heterogeneity in the same tumour type [19,21,22].

In the present study, the slope of the γH2AX foci dose–response curve was investigated with regard to its predictive value for radiosensitivity in a micromilieu dependent manner in seven well established *in vivo* HNSCC models with known radiosensitivity (radioresistant, intermediate, radiosensitive). The slopes of the γH2AX foci dose–response curves of surgically removed and *ex vivo* irradiated clinical HNSCC specimens were then used to group samples into radioresistant, intermediate, and radiosensitive tumours according to the *in vivo* results.

Material and methods

Tumour models and in vivo γH2AX foci assay

Seven well established and previously described squamous cell carcinoma cell lines (FaDu, SAS, SKX, UT-SCC-5, UT-SCC-14, UT-SCC-45, XF354) were used for this study [18,23–25]. Biological constancy of the tumour models was verified by microsatellite analyses at the last passage before transplantation. Seven to fourteen-week-old male and female NMRI (nu/nu) mice were used as tumour hosts. The mice were maintained in a pathogen-free animal breeding facility (OncoRay, Dresden) with a cycle of 12 h of light and 12 h of dark and were fed *ad libitum*. The animal facilities and the experiments were approved according to institutional guidelines and the German animal welfare regulations. For further immunosuppression, the animals received a 4 Gy whole body irradiation 2–4 days before tumour transplantations. All irradiations were performed with 200 kV X-rays (Isovolt 320/13, Seifert, Ahrensdorf, Germany; 20 mA; 0.5 mm Cu filter; dose rate 1 Gy/min), and antibiotics were added to the drinking water for 10 days to prevent infection. For each tumour model, tumour pieces were transplanted subcutaneously to the hindleg of 50 anaesthetised mice (120 mg/ kg ketamine [intraperitoneal, i.p.], Rompun, Bayer Health Care, GmbH, Germany and 16 mg/kg xylazine i.p., ketamine 500, Curamed, Curamed Pharma, Germany). Tumour growth was monitored weekly with a caliper. When the tumour reached a size of 7 × 7 mm, BrdU (proliferation/viability marker, 3.75 mg, SERVA electrophoresis, Heidelberg, Germany) and pimonidazole (hypoxia marker, 0.1 mg/g body weight, HPI, Inc, Burlington, MA, USA) were injected intraperitoneally.

One hour after injection, the mice were randomly assigned to the five treatment arms: unirradiated control, irradiation with 2, 4, 6, or 8 Gy under ambient blood flow.

Tumours were excised 24 h post irradiation and fixed in 4% formalin before embedding in paraffin.

Patient material

Head and neck cancer samples were obtained with patient consent from the Department of Otorhinolaryngology, Faculty of Medicine and University Hospital Carl Gustav Carus, Technische Universität Dresden, Germany between 2014 and 2017. For this study, 15 patients' samples were processed for the evaluation of γH2AX foci. Inclusion criteria were sufficient tumour material (approximately 1 cm^3) to perform the assay and no other treatment intervention, e.g. chemo- or radiotherapy, prior to surgery. Patients were included independently of gender, age, comorbidities, tumour stage, grade, or tumour location in head and neck region. The only female patient was re-classified as a malignant melanoma of the nasal cavity, this sample was omitted in the analyses of the correlations with the clinical parameters. Human Papillomavirus (HPV) status was systematically assessed with an LCD-Array HPV kit [26]. A pseudonym was attributed for each patient and information relative to their diagnosis and treatment were compiled in the RadPlanBio platform [27]. The patient study was approved by the local ethics committee (EK152052013).

Upon receipt in DMEM medium (Biochrom GmbH, Berlin, Germany), the material was processed within 1 h. The tissue was rinsed in sodium chloride solution (NaCl, Fresenius Kabi, Germany) and one piece was fixed in 4% formalin for embedding.

The γH2AX *ex vivo* foci assay has previously been described [21]. In brief, depending on the quantity of provided sample, 4 to 8 specimens of ~4–12 mm^3 were reoxygenated at 37 °C in DMEM medium supplemented with antibiotics in an agarose-coated petri dish for 24 h. During the last 4 h of incubation, the medium was supplemented with BrdU and pimonidazole to assess the micromilieu. Subsequently, the specimens were irradiated with 0, 2, 4, or 8 Gy with 200 kV X-rays (Isovolt 320/13, Seifert, Ahrensdorf, Germany; 20 mA; 0.5 mm Cu filter; dose rate 1 Gy/min). The medium was exchanged after irradiation, and the specimens were incubated for 24 h. Finally, the samples were fixed in 4% formalin and processed for histological analysis.

γH2AX and micromilieu markers (BrdU; pimonidazole) staining and evaluation

The staining protocols have previously been described [18]. Briefly, two consecutive 3 μm sections from the tumour were stained for γH2AX, 4′, 6-diamidino-2-phenylindole (DAPI, 1 μM) and BrdU/pimonidazole.

The AxioImagerM1 (Carl Zeiss, Jena, Germany) was used for evaluation of the stainings. The immunohistochemistry sections were scanned with a colour camera (Axiocam MRc, Carl Zeiss, Jena, Germany, 100X) and 10–15 regions of interest were marked relative to the micromilieu parameter. For each region of interest (ROI), immunofluorescence images were acquired on 17 focal planes being 0.25 μm apart (Z-stacks) with a monochrome camera (Axiocam MRm, Carl Zeiss, Jena, Germany; motorized scanning stage, Maerzhaeuser, Wetzlar, Germany, 400X). The Z-stacks images were fused to a single image for analysis. For the *in vivo* protocol, γH2AX foci were evaluated in viable cell nuclei located in oxygenated areas with a maximal distance of 45 μm to the closest perfused vessel [18]. For each tumour, 50 randomly selected nuclei distributed over 10 ROI were analysed (γH2AX foci, nucleus area, distance to the vessel) by a blinded observer. For the *ex vivo* protocol, viable areas were assessed in the immunohistochemistry sections by an absence of pimonidazole, a presence of BrdU positive cell nuclei and by morphology of the cells. When minimal BrdU was present in the tissue sections, due to e.g. slow proliferation, the tumour was considered viable when the tissue was homogeneous, and no histological sign of necrosis could be observed. Oxic areas were typically present at the rim of the sample, whereas the tissue core appeared to be positive to pimonidazole. Depending on the tumour content and the size of the clinical sample, 3–20 ROI/specimens could be evaluated. The corresponding fields were identified in the immunofluorescence stained consecutive section. Hypoxic areas were marked by superimposing immunofluorescence and immunohistochemistry images with Adobe Photoshop (Adobe Systems, San Jose, California). In each ROI, 2–20 randomly selected nuclei were analysed for γH2AX foci and the nucleus area. All annotations were performed with AxioVision software (Zeiss).

Statistical analysis

As the residual foci are evaluated on paraffin section, where only a portion of cell nucleus is present, calculations were made in relation to the nucleus areas.

normalised foci (*nfoci*) were calculated according to the formula modified from [19]:

1) $cfoci_{dose} = Am/Ai * foci_{dose}$
2) $nfoci_{dose} = cfoci_{dose} - cfoci_0$

where the number of counted foci ($foci_{dose}$) was divided by the area of the individual nucleus (*Ai*) and multiplied by an overall area (*Am*) of the tumour model or patient specimen to account for difference in the cell cycle, general DNA content and packing density, and allow comparison between the different models 1). The overall area (*Am*) was calculated for each dose group to account for the increase in mean area that was observed in irradiated tumours compared to unirradiated tumours (Supp. Figs. 1, 2). The mean *cfoci* value from the control tumours (no irradiation) was subtracted from each value to account for basal foci which are not attributed to irradiation 2). Negative nfoci values after subtraction were set to zero assuming that irradiation causes DNA damages ≥zero. Analyses were performed with Excel, SPSS 25 (Statistical Package for the Social Sciences – IBM, Armonk, New York) and R (R Foundation for Statistical Computing, Vienna, Austria, version 3.3.2). The coefficient of variation (CV) was calculated as:

$$CV = SD/mean * 100$$

where SD is the standard deviation of the foci values.

The TCD_{50} values used for correlation were previously published [18].

Results

Fig. 1A shows the workflow of the pre-clinical *in vivo* study, in which seven HNSCC xenografts models (Table 1) were irradiated with 2, 4, 6, or 8 Gy and γH2AX foci were evaluated in a micromilieu dependent manner (Fig. 1B). There was no pronounced saturation of the γH2AX signal at high doses, and discrete foci could be evaluated at 6 and 8 Gy in every tumour model. The characteristics of the HNSCC models are given in Table 1.

Statistical analyses revealed a significant increase in cell nucleus areas size with increasing irradiation dose in all the models (except for UT-SCC-5 and SAS at 2 Gy, Supp. Figs. 1 and 2). Consequently, the nucleus areas of each dose group were used for normalisation. Linear regression analysis showed that the distance to the vessel had no major influence on γH2AX foci distribution within a distance of 45 μm from the vessel [18, 23, Supp. Fig. 3]. Further, no significant correlation was observed between the distance to the vessel and the nuclear size in most cases within this distance (Supp. Fig. 4).

Fig. 1C shows representative images of the increasing residual γH2AX signal following irradiation. The γH2AX foci in unirradiated tumours (endogenous or basal foci) showed distinct differences in the models (Fig. 1D). The HPV positive and radiation sensitive model UT-SCC-45 had the highest amount of basal foci (12.3 ± 1.3 cfoci/nucleus) whereas the intermediate resistant model FaDu had the lowest background foci number (1.4 ± 0.3 cfoci/nucleus). However, no significant correlation could be identified between the basal cfoci value and the $TCD_{50,fx}$ ($p = 0.30$) or with the $TCD_{50,SDclamp}$ ($p = 0.79$).

Linear regression analyses showed that the number of nfoci increases significantly in a dose dependent manner in every model ($p < 0.05$, Fig. 1E, Table 1). A significant correlation (Pearson's) between nfoci values at 6 Gy and the $TCD_{50,fx}$ ($p = 0.03$), as well as nfoci at 8 Gy and both the $TCD_{50,fx}$ ($p = 0.04$) and the $TCD_{50,SD,clamp}$ ($p = 0.02$) could be found. Lower individual doses did not present any significant correlation with the TCD_{50} values (data not shown). The slopes of the residual nfoci dose–response curves ranged from 0.329 Gy^{-1} (UT-SCC-5) to 1.320 Gy^{-1} (SKX) and negatively correlated with the $TCD_{50,fx}$ ($R^2 = 0.63$, $p = 0.032$) and with the $TCD_{50,SD,clamp}$ ($R^2 = 0.66$, $p = 0.027$) (Fig. 1F and G).

The workflow for the clinical *ex vivo* γH2AX assay [19] and representative images are shown in Fig. 2A, B and C. The exclusively male HNSCC patient cohort had a mean age of 65.4 years (Table 2). Sample #4 tested positive for HPV (subtype 33). Inter-patient variability was detected for BrdU incorporation and hypoxia (data not shown), and endogenous cfoci (Fig. 2D); the latter range from 0.5 ± 0.1 cfoci/nucleus in sample #11 to 5.1 ± 0.3 cfoci/nucleus in sample #2 (CV = 51.5%, variation of 10-fold in the samples). The nucleus areas were investigated and neither a systematic increase with the dose nor a correlation of the nucleus areas with the clinical parameters could be observed in the patients' samples (data not shown). Concerning the γH2AX assay, the nfoci value increased linearly with the dose ($p < 0.05$), except in samples #7 and #5 (p-value = 0.06). The slopes of the nfoci dose–response curve ranged from 0.1 ± 0.03 Gy^{-1} in #7 to 0.9 ± 0.08 Gy^{-1} in #9 (CV 52.8%, 9-fold difference, Fig. 2E, Table 2). Significant correlations between patient's age and slope of the residual nfoci dose–response curves ($p < 0.001$) as well as nfoci at 8 Gy ($p < 0.001$) were found (Fig. 2 F and G). Tumour grade, T stage and N stage were not associated with slope or nfoci except for T stage and nfoci at 4 Gy ($p = 0.026$) with smaller tumours (T1, T2) presenting more foci than more advanced tumours (T3, T4, Tx) (Fig. 2H). Two samples presenting a low BrdU level (samples #6 and #10) were included in the analysis. Statistical testing revealed minimal changes in the analyses when these samples were removed from the analysis, and the same conclusion could be drawn (Supp. Fig. 5).

The *in vivo* pre-clinical study showed that residual nfoci after 8 Gy and the slope of the dose–response curve were good predictors for radiosensitivity. Therefore, the slopes of the residual nfoci dose–response curves of the patients' samples were grouped according to the slopes of the xenografts' dose–response curves. The three groups consisted in a radiosensitive (slope >0.7 Gy^{-1}; four patients SKX, UT-SCC-45), intermediate resistant (slope 0.4–0.7 Gy^{-1}; five patients, FaDu, UT-SCC-14, XF354) and radioresistant (slope <0.4 Gy^{-1}; five patients, SAS, UT-SCC-5) group (Fig. 3) which were statistically significantly different ($p <= 0.001$). The values of nfoci (8 Gy) significantly correlated with the slopes ($R^2 = 0.98$, $p < 10^{-10}$) and grouping of patient's samples according to nfoci at 8 Gy leads to similar group assignment.

Discussion

This study evaluated the slope of the dose–response curve (0–8 Gy) measured with γH2AX nfoci as a predictor for local tumour control in seven well established HNSCC models with differences in intrinsic radiosensitivity. The micromilieu was considered, as it is well known that the oxygen status influences DNA damage, and consequently, γH2AX foci [23,28]. In every pre-clinical tumour model, an increase in nucleus area size was detected with increasing irradiation dose. Equivalent results have been gathered in other models, and this increase was attributed to changes in cell cycle repartition and a blockage of the cells in G2 [29]. Following 2 Gy irradiation, the cell nucleus area was unaffected in the most radioresistant models SAS and UT-SCC-5. In the clinical samples however, no systematic areas increase could be detected. This might be attributed to the assay setting of *in vivo* and *ex vivo* exposure.

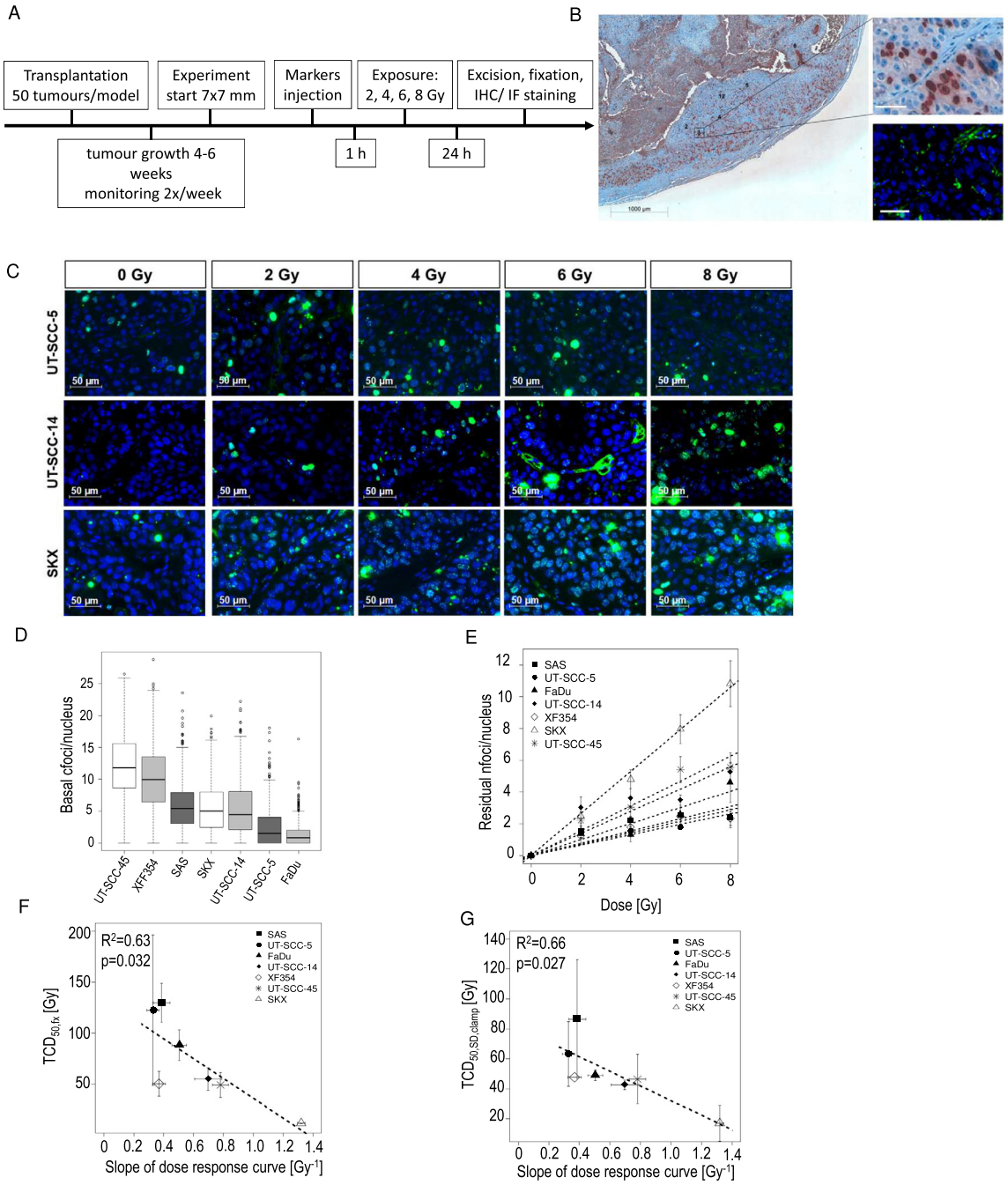

Fig. 1. The pre-clinical *in vivo* γH2AX assay in seven HNSCC models. (A) Workflow of the experiment. Tumour pieces were transplanted to the hindleg of NMRI nude mice and monitored weekly until they reached 7 × 7 mm. Biological markers (BrdU for cell proliferation/viability; pimonidazole for hypoxia) were injected 1 h prior to irradiation. Tumours were irradiated with 0, 2, 4, 6, or 8 Gy respectively and excised 24 h post irradiation. (B) Representative images of immunohistochemistry (IHC) and immunofluorescence (IF) in FaDu. 10–15 fields were randomly selected based on the cell viability, hypoxia and presence of a perfused vessel. Respective fields were searched for in the corresponding IF picture (γH2AX foci (green) and DNA (DAPI, blue)). Scale bar 50 µm (C) Exemplary images of fluorescence stained tumour sections of the models UT-SCC-5, UT-SCC-14 and SKX irradiated with 0, 2, 4, 6, or 8 Gy showing a dose dependent increase in residual γH2AX foci. (D) Basal foci ± SEM in the 7 HNSCC models (white: radiosensitive models; grey: intermediate models; dark grey: radioresistant). (E) Dose–response curve of the residual nfoci ± SEM. (F,G) The slopes of the dose–response curve ± SEM of the established HNSCC models correlate with the TCD_{50} (F) following fractioned irradiation over 6 weeks ($TCD_{50,fx}$) and (G) following single dose exposure ($TCD_{50,SD}$). The results of the linear regression are presented on the graphics (coefficient of determination R^2 and the *p*-value).

In the pre-clinical study, we observed that the HNSCC models present different amount of basal and residual γH2AX foci. Residual γH2AX foci were found to increase linearly with the dose, and the slopes values ranged from 0.329 Gy^{-1} to 1.320 Gy^{-1}. The slopes of the residual γH2AX nfoci as well as the individual nfoci after 6 and 8 Gy negatively correlated with the $TCD_{50,fx}$ and the $TCD_{50,SD,clamp}$, while lower doses (2 and 4 Gy) showed no correlation. A similar observation was made in lymphocytes from breast cancer patients [30]. The correlation between acute risk effect and radiosensitivity was observed after 6 Gy, but not after 3 Gy irradiation. In contrast, in a previous report, a correlation of nfoci after 4 Gy irradiation with the TCD_{50} was found [18] which might be attributed to the lower number of analysed models in the current study. Higher doses might be more appropriate to distinguish

Table 1
Characteristics of the HNSCC xenograft models.

Tumour model	Anatomical site	Grade	$TCD_{50,SD,clamp}$ (Gy) +/− Variance	$TCD_{50,Fx}$ (Gy) +/− Variance	Slope dose–response curve (Gy^{-1})	SEM	R^2	*p*-Value	Radiosensitivity based on TCD_{50}
SAS	Tongue	G4	86.4 ± 39.81	129.8 ± 19.25	0.386	0.056	0.92	0.002	Resistant
UT-SCC-5	Tongue	G3	63.3 ± 21.72	122.3 ± 73.91	0.329	0.040	0.94	0.012	
FaDu	Hypopharynx	G4	49.0 ± 3.53	88.3 ± 15.19	0.505	0.048	0.96	0.005	Intermediate
UT-SCC-14	Tongue	G3	42.7 ± 3.28	55.2 ± 10.97	0.697	0.090	0.94	0.002	
XF354	Floor of the mouth	G3	47.7 ± 202.21	50.4 ± 11.99	0.368	0.043	0.95	0.001	
UT-SCC-45*	Floor of the mouth	G4	46.5 ± 16.50	49.3 ± 11.99	0.781	0.055	1.00	$<10^{-6}$	Sensitive
SKX§	Floor of the mouth and alveolar bone	G2	16.9 ± 12.03	11.76 ± 0.17	1.320	0.026	0.98	$<10^{-4}$	

The models were grouped as resistant, intermediate and sensitive according to the TCD_{50}. *HPV positive, §repair deficient, G grade, SEM standard error of the mean, R^2 coefficient of determination, TCD_{50} tumour control dose 50%, radiation dose to locally control 50% of the tumours, SD single dose. The TCD_{50} were published in [18]. The features of the HNSCC models were previously presented in [18], 23–25.

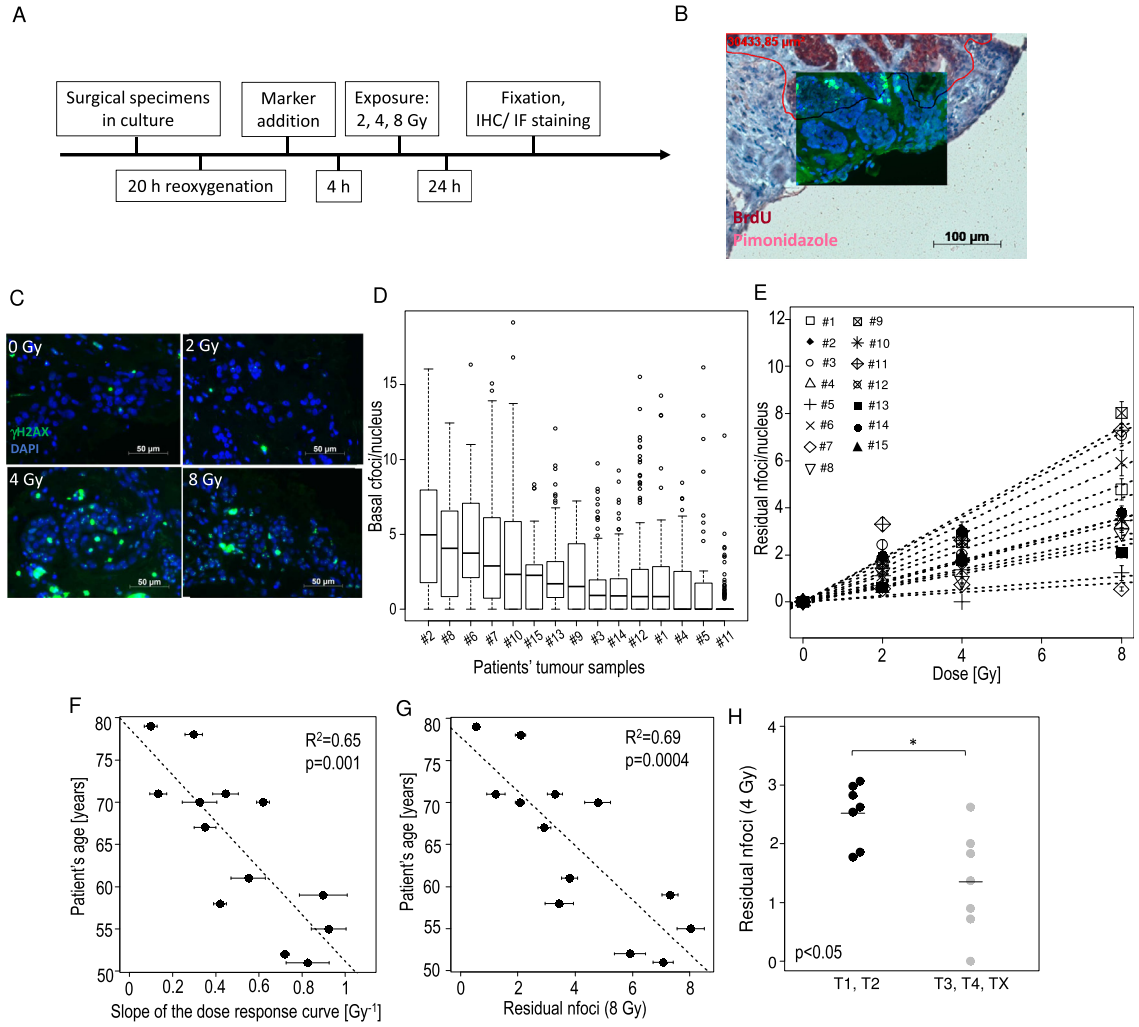

Fig. 2. The *ex vivo* γH2AX assay with the patients' samples. (A) Workflow of the clinical *ex vivo* γH2AX foci assay. (B) Overlay of the IHC and the IF images. Fields were analysed at the rim of the tumour sample in oxic (pimonidazole negative) and viable areas (BrdU positive). (C) Exemplary IF images of a HNSCC patient's sample irradiated with 0, 2, 4, or 8 Gy showing residual foci in the patient materials. (D) Patient specific basal foci in the clinical samples. (E) Dose–response curves of patients' specimens following *ex vivo* irradiation. (F) The slope of the dose–response curve ± SE is influenced by the age of the patient. (G) nfoci (8 Gy) ± SE is influenced by the age of the patient. The results of the linear regression are presented on the graphics (coefficient of determination R^2 and the *p*-value). (H) Samples grouped by T stage and nfoci (4 Gy), $^*p < 0.05$ (Mann–Whitney test).

intrinsic radiosensitivity. Nevertheless, additional analyses including more models and counts are required to draw a solid conclusion.

The *ex vivo* γH2AX assay was previously described for tumour samples originating from HNSCC xenografts and for non-HNSCC patients' specimens [19,21,22,31]. The present study demonstrates that the assay is feasible in clinical specimens originating from head and neck cancers. Residual foci were analysed in 1–2 biopsies/dose depending on the amount of available material. Intra-tumoural heterogeneity is beyond the scope of this study;

Table 2
Characteristics of the patients' samples.

Sample	Patient ID	Gender	Age	T	N	M	Grade	Tumour location	Linear regression analysis				Radiosensitivity based on slope
									Slope (Gy^{-1})	SE	R^2	*p*-Value	
#7	OR_HNSCC_P3DRVYTC	m	79	pTx	pNx	M0	G2	Parotid gland	0.10	0.03	0.73	0.064	Resistant
#5	OR_HNSCC_X0GVY0E4	m	71	TX	pN2a (1/19)		G2	Lymph node metastasis (parotide)	0.13	0.04	0.76	0.055	
#13	OR_HNSCC_PKKGFMCE	m	78	pT2	pN0	cM0	G3	Base of the tongue	0. 30	0.04	0.95	0.005	
#12	OR_HNSCC_0J2ZH7JM	m	70	cT4a	cN0	cM0		Oropharynx	0.33	0.08	0.84	0.029	
#8	OR_HNSCC_P3P0G4ZP	m	67	pT3	pN1 (1/34)	M0		Oropharynx, tongue, tonsils, parapharyngeal and masticator area	0.35	0.05	0.95	0.005	
#10	OR_HNSCC_H1Z6ETK8	m	58	T4a	N2 (1/29)	M0	G3	Piriform sinus	0.42	0.03	0.99	$<10^{-3}$	Intermediate
#15*	OR_HNSCC_7M7RHKGV	f	78	T2	N1	M0		Nasal cavity (malignant melanoma)	0.42	0.05	0.97	0.014	
#4§	OR_HNSCC_2HGM2FQA	m	71	pT2	pN2b (3/41)	cM0	G3	Tonsils	0.45	0.06	0.94	0.006	
#14	OR_HNSCC_92TH1W23	m	61	pT2	pN2b (2/12)	cM0	G3	Floor of the mouth	0.55	0.08	0.94	0.007	
#1	OR_HNSCC_KH3AA05Q	m	70	pT1	pN0 (0/27)		G3	Hypopharynx and soft palate	0.62	0.03	1.00	0.002	
#6	OR_HNSCC_3J326F82	m	52	cT4	cN2c	cM0	G3	Hypopharynx/oropharynx/larynx	0.72	0.02	1.00	$<10^{-4}$	Sensitive
#3	OR_HNSCC_M0FRH0JE	m	51	pT4a	pN2b(3/88)	cM0	G3	Larynx	0.83	0.10	0.96	0.004	
#11	OR_HNSCC_Q00N2D11	m	59	pT2	pN2	cM0		Tongue (edge)	0.90	0.11	0.96	0.004	
#9	OR_HNSCC_2L05VHJ0	m	55	T2	N2c (4/57)	M0	G2	Soft palate	0.92	0.08	0.98	0.002	
#2	OR_HNSCC_JH3K67HG	m	61	pT1	pN2 (1/34)/pN2a (1/14)	cM0	G2	Floor of the mouth/Vallecula epiglottica					Non assignable due to minimal sample

Clinical parameters of the patient's cohort recruited for the *ex vivo* γH2AX assay. The information was provided by the pathology department m: male, f: female, TNM status: T (tumour size), N (lymph node metastasis), M (distant metastasis), c: clinical evaluation, p: histopathological evaluation, G: grade, blank: information not available. The HPV (Human Papillomavirus) status was tested in every sample, *Denotes a melanoma § denotes the only HPV+ sample. The samples were grouped as resistant, intermediate and sensitive based on their slopes. SE: standard error, R^2 coefficient of determination.

however, recent studies support the hypothesis that one biopsy is sufficient to accurately estimate the foci number and infer radiosensitivity [22,32].

A linear dose–response relationship was detected with residual foci, with slopes ranging from 0.099 Gy^{-1} to 0.920 Gy^{-1}. A high inter-patient variability was observed for the endogenous γH2AX cfoci, residual γH2AX nfoci as well as the slopes of the residual γH2AX nfoci dose–response curve (Fig. 2.D, E, table 2). Inter-individual variability has also been described by others [33,34] and suggests different DNA repair mechanism capacities and a potential for treatment individualisation.

Endogenous or basal foci represent DNA damage in untreated cells [35] and have been associated with genomic instability; a common feature of cancer [36]. Linear regression analysis did not reveal any correlation between basal nfoci and the TCD_{50} which is consistent with other studies [15,18,36].

The development of HNSCC may be caused by HPV infection [37]. Patients with HPV positive oropharyngeal tumours typically respond better to radiotherapy [38], which is discussed to be attributed to impaired DNA damage repair and immune response [39,40]. Data on HPV infection status and presence of γH2AX are contradictory. While some studies showed that the presence of HPV (subtype 16) led to a higher proportion of cells with basal γH2AX foci [15,41], other studies report a low amount of γH2AX foci in a subset of HPV positive cell lines [36]. Among the seven pre-clinical HNSCC models, only UT-SCC-45 is HPV positive (subtype 33). This model showed a high amount of basal γH2AX as well as an increased radiosensitivity indicated by a slope of 0.78 Gy^{-1}. In the current patients' cohort, only one sample is HPV positive (#4, subtype 33). Neither the basal foci nor the slope of the dose–response curve was increased for this sample. Further study is required to draw a solid conclusion as to the interplay between γH2AX foci, HPV infection status and radiosensitivity.

In the pre-clinical study, it was shown that the slope of the dose–response curve was a good predictor of radiosensitivity. The patient derived HNSCC samples were hence grouped according to the slopes of the dose–response curves. Based on the *in vivo* results, it can be speculated that the group 1 [slope s < 0.40] corre-

Fig. 3. Classification of the patients' samples based on the slopes of the dose–response curve. Filled circles represent patients' samples, open squares represent the pre-clinical HNSCC models. The groups were compared with the Mann–Whitney test, $^{***}p < 0.001$; $^{**}p < 0.01$, $^{*}p < 0.05$.

sponds to radioresistant tumours, the samples with a slope [0.40–0.70] are intermediate, and the samples with s >0.70 are radiosensitive. Currently, relevant clinical parameters such as the local tumour control or overall survival at 5 years are not available for all analysed patients, which prevents the verification of patient grouping. However, a significant negative correlation was found for the slope of the nfoci dose–response curve and the patients' age at diagnosis [51–79 y.o.; Fig. 2F]. A similar negative correlation between residual γH2AX foci measured with the RABiT (Rapid Automated Biodosimetry Tool) and 4 Gy-irradiated lymphocytes of 94 healthy donors at the age of 21 to 50 was shown [42]. As cancer risk increases with age, patients diagnosed with cancer at a younger age might be prone to cancer due to defects in repair mechanisms or mutations in oncogenes. Further investigation is required to uncover the relationship between the age of the patients and the damage repair capacity and radiosensitivity. This observation might be relevant for treatment optimisation, although previous studies report a lack of association between the age of the patient and the outcome after radiotherapy treatment in head and neck cancers [43].

This study further supports the validity of residual γH2AX foci to assess radiosensitivity in head and neck cancers. The slope of the dose–response curve was found to be a good predictor for radiosensitivity in pre-clinical tumour models. As it considers different samples irradiated at different doses, it might be more robust than single values. Nonetheless, the nfoci at 8 Gy, which was also found to predict the local tumour control, could be used in case of low amount of material. The transfer to clinical samples in an *ex vivo* setting showed that the assay is feasible in head and neck cancers and revealed inter-patient variability. Provided that this inter-patient variability is associated with different responses to radiation, residual γH2AX foci could be evaluated prior to treatment to optimise the dose delivered and treat the patients based on their individual features.

Funding

This work was supported by the Federal Ministry of Education and Research (BMBF 02NUK035C).

Conflict of interest

None.

Acknowledgement

The authors thank the Clinical Trial Unit of the Faculty of Medicine of the TU Dresden, the physicians for recruiting patients and the patients for agreeing to donate samples for the study. The authors acknowledge K. Schumann, E. Jung, D. Pfitzmann, A. Kluske, S. Balschukat, L. Stolz-Kieslich, D. Friede and N. v. Auw for the technical support.

Appendix A. Supplementary data

Supplementary data to this article can be found online at https://doi.org/10.1016/j.radonc.2019.04.009.

References

[1] Borras JM, Lievens Y, Dunscombe P, Coffey M, Malicki J, Corral J, et al. The optimal utilization proportion of external beam radiotherapy in European countries: An ESTRO-HERO analysis. Radiother Oncol 2015;116:38–44.
[2] Fertil B, Malaise E-P. Inherent cellular radiosensitivity as a basic concept for human tumour radiotherapy. Int J Radiat Oncol Biol Phys 1981;7:621–9.
[3] Caudell JJ, Torres-Roca JF, Gillies RJ, Enderling H, Kim S, Rishi A, et al. The future of personalised radiotherapy for head and neck cancer. Lancet Oncol 2017;18:e266–73.
[4] Baumann M, Krause M, Overgaard J, Debus J, Bentzen SM, Daartz J, et al. Radiation oncology in the era of precision medicine. Nat Rev Cancer 2016;16:234–49.
[5] Begg AC. Predicting response to radiotherapy: Evolutions and revolutions. Int J Radiat Biol 2009;85:825–36.
[6] Ferlay J, Steliarova-Foucher E, Lortet-Tieulent J, Rosso S, Coebergh JWW, Comber H, et al. Cancer incidence and mortality patterns in Europe: Estimates for 40 countries in 2012. Eur J Cancer 2013;49:1374–403.
[7] Gatta G., Botta L., Sánchez M.J., Anderson L.A., Pierannunzio D., Licitra L., 2015. Prognoses and improvement for head and neck cancers diagnosed in Europe in early 2000s: The EUROCARE-5 population-based study. European Journal of Cancer, Survival of Cancer Patients in Europe, 1999–2007: The EUROCARE-5 Study 51, 2130–2143.
[8] Rogakou EP, Boon C, Redon C, Bonner WM. Megabase chromatin domains involved in DNA double-strand breaks in vivo. J Cell Biol 1999;146:905–16.
[9] Rogakou EP, Pilch DR, Orr AH, Ivanova VS, Bonner WM. DNA double-stranded breaks induce histone H2AX phosphorylation on serine 139. J Biol Chem 1998;273:5858–68.
[10] Rothkamm K, Löbrich M. Evidence for a lack of DNA double-strand break repair in human cells exposed to very low x-ray doses. PNAS 2003;100:5057–62.
[11] Sedelnikova OA, Rogakou EP, Panyutin IG, Bonner WM. Quantitative detection of (125)IdU-induced DNA double-strand breaks with gamma-H2AX antibody. Radiat Res 2002;158:486–92.
[12] Banáth JP, Klokov D, MacPhail SH, Banuelos CA, Olive PL. Residual γH2AX foci as an indication of lethal DNA lesions. BMC Cancer 2010;10.
[13] Olive PL. Retention of γH2AX foci as an indication of lethal DNA damage. Radiother Oncol 2011;101:18–23.
[14] Taneja N, Davis M, Choy JS, Beckett MA, Singh R, Kron SJ, et al. Histone H2AX phosphorylation as a predictor of radiosensitivity and target for radiotherapy. J Biol Chem 2004;279:2273–80.
[15] Banáth JP, MacPhail SH, Olive PL. Radiation sensitivity, H2AX phosphorylation, and kinetics of repair of DNA strand breaks in irradiated cervical cancer cell lines. Cancer Res 2004;64:7144–9.
[16] Olive PL, Banáth JP. Phosphorylation of histone H2AX as a measure of radiosensitivity. Int J Radiat Oncol Biol Phys 2004;58:331–5.
[17] Klokov D, MacPhail SM, Banáth JP, Byrne JP, Olive PL. Phosphorylated histone H2AX in relation to cell survival in tumour cells and xenografts exposed to single and fractionated doses of X-rays. Radiother Oncol 2006;80:223–9.
[18] Koch U, Höhne K, von Neubeck C, Thames HD, Yaromina A, Dahm-Daphi J, et al. Residual γH2AX foci predict local tumour control after radiotherapy. Radiother Oncol 2013;108:434–9.
[19] Menegakis A, De Colle C, Yaromina A, Hennenlotter J, Stenzl A, Scharpf M, et al. Residual γH2AX foci after ex vivo irradiation of patient samples with known tumour-type specific differences in radio-responsiveness. Radiother Oncol 2015;116:480–5.
[20] Menegakis A, Yaromina A, Eicheler W, Dörfler A, Beuthien-Baumann B, Thames HD, et al. Prediction of clonogenic cell survival curves based on the number of residual DNA double strand breaks measured by γH2AX staining. Int J Radiat Biol 2009;85:1032–41.
[21] Menegakis A, von Neubeck C, Yaromina A, Thames H, Hering S, Hennenlotter J, et al. γH2AX assay in ex vivo irradiated tumour specimens: A novel method to determine tumour radiation sensitivity in patient-derived material. Radiother Oncol 2015;116:473–9.
[22] De-Colle C, Yaromina A, Hennenlotter J, Thames H, Mueller A-C, Neumann T, et al. Ex vivo γH2AX radiation sensitivity assay in prostate cancer: Inter-patient and intra-patient heterogeneity. Radiother Oncol 2017;124(3):386–94.
[23] Menegakis A, Eicheler W, Yaromina A, Thames HD, Krause M, Baumann M. Residual DNA double strand breaks in perfused but not in unperfused areas determine different radiosensitivity of tumours. Radiother Oncol 2011;100:137–44.
[24] Yaromina A, Krause M, Thames H, Rosner A, Krause M, Hessel F, et al. Pre-treatment number of clonogenic cells and their radiosensitivity are major determinants of local tumour control after fractionated irradiation. Radiother Oncol 2007;83:304–10.
[25] Yaromina A, Thames H, Zhou X, Hering S, Eicheler W, Dörfler A, et al. Radiobiological hypoxia, histological parameters of tumour microenvironment and local tumour control after fractionated irradiation. Radiother Oncol 2010;96:116–22.
[26] Lohaus F, Linge A, Tinhofer I, Budach V, Gkika E, Stuschke M, et al. HPV16 DNA status is a strong prognosticator of loco-regional control after postoperative radiochemotherapy of locally advanced oropharyngeal carcinoma: Results from a multicentre explorative study of the German Cancer Consortium Radiation Oncology Group (DKTK-ROG). Radiother Oncol 2014;113:317–23.
[27] Skripcak T, Belka C, Bosch W, Brink C, Brunner T, Budach V, et al. Creating a data exchange strategy for radiotherapy research: Towards federated databases and anonymised public datasets. Radiother Oncol 2014;113:303–9.
[28] Olive PL, Banuelos CA, Durand RE, Kim J-Y, Aquino-Parsons C. Endogenous and radiation-induced expression of γH2AX in biopsies from patients treated for carcinoma of the uterine cervix. Radiother Oncol 2010;94:82–9.
[29] Skog S, Tribukait B. Cell size following irradiation in relation to cell cycle. Acta Radiol Oncol 1986;25:269–73.

[30] Borgmann K, Hoeller U, Nowack S, Bernhard M, Röper B, Brackrock S, et al. Individual radiosensitivity measured with lymphocytes may predict the risk of acute reaction after radiotherapy. Int J Radiat Oncol Biol Phys 2008;71:256–64.
[31] Rassamegevanon T, Löck S, Range U, Krause M, Baumann M, von Neubeck C. Tumour heterogeneity determined with a γH2AX foci assay: A study in human head and neck squamous cell carcinoma (hHNSCC) models. Radiother Oncol 2017;124:379–85.
[32] Rassamegevanon T, Löck S, Baumann M, Krause M, von Neubeck C. Heterogeneity of γH2AX foci increases in ex vivo biopsies relative to in vivo tumours. Int J Mol Sci 2018;19:2616.
[33] Ismail IH, Wadhra TI, Hammarsten O. An optimized method for detecting gamma-H2AX in blood cells reveals a significant interindividual variation in the gamma-H2AX response among humans. Nucleic Acids Res 2007;35(5):e36.
[34] Bañuelos CA, Banáth JP, Kim J-Y, Aquino-Parsons C, Olive PL. gammaH2AX expression in tumours exposed to cisplatin and fractionated irradiation. Clin Cancer Res 2009;15:3344–53.
[35] Paull TT, Rogakou EP, Yamazaki V, Kirchgessner CU, Gellert M, Bonner WM. A critical role for histone H2AX in recruitment of repair factors to nuclear foci after DNA damage. Curr Biol 2000;10:886–95.
[36] Yu T, MacPhail SH, Banáth JP, Klokov D, Olive PL. Endogenous expression of phosphorylated histone H2AX in tumours in relation to DNA double-strand breaks and genomic instability. DNA Repair 2006;5(8):935–46.
[37] Gillison ML, Koch WM, Capone RB, Spafford M, Westra WH, Wu L, et al. Evidence for a causal association between human papillomavirus and a subset of head and neck cancers. J Natl Cancer Inst 2000;92:709–20.
[38] Lassen P, Eriksen JG, Hamilton-Dutoit S, Tramm T, Alsner J, Overgaard J. Effect of HPV-associated p16INK4A expression on response to radiotherapy and survival in squamous cell carcinoma of the head neck. JCO 2009:1992–8.
[39] Rieckmann T, Tribius S, Grob TJ, Meyer F, Busch C-J, Petersen C, et al. HNSCC cell lines positive for HPV and p16 possess higher cellular radiosensitivity due to an impaired DSB repair capacity. Radiother Oncol 2013;107:242–6.
[40] Ward MJ, Thirdborough SM, Mellows T, Riley C, Harris S, Suchak K, et al. Tumour-infiltrating lymphocytes predict for outcome in HPV-positive oropharyngeal cancer. Br J Cancer 2014;110:489–500.
[41] Duensing S, Münger K. The human papillomavirus type 16 E6 and E7 oncoproteins independently induce numerical and structural chromosome instability. Cancer Res 2002;62:7075–82.
[42] Sharma PM, Ponnaiya B, Taveras M, Shuryak I, Turner H, Brenner DJ. High throughput measurement of γH2AX DSB repair kinetics in a healthy human population. PLoS One 2015;10.
[43] Pignon T, Horiot J-C, den Bogaert WV, Glabbeke MV, Scalliet P. No age limit for radical radiotherapy in head and neck tumours. Eur J Cancer 1996;32:2075–81.